Structure, Vol. 11, 225–236, February, 2003, ©2003 Elsevier Science Ltd. All rights reserved. PII S0969-2126(03)00011-X

Alternative Conformations of HIV-1 V3 Loops Mimic β Hairpins in Chemokines, Suggesting a Mechanism for Coreceptor Selectivity

Michal Sharon,[1] Naama Kessler,[1] Rina Levy,[1] Susan Zolla-Pazner,[2] Matthias Görlach,[3] and Jacob Anglister[1,*]

[1]Department of Structural Biology
The Weizmann Institute of Science
Rehovot 76100
Israel

[2]New York VA Medical Center and
New York University School of Medicine
New York, New York 10010

[3]Department of Molecular Biophysics/NMR Spectroscopy
Institute for Molecular Biotechnology (IMB)
Beutenbergstrasse 11
D-07745 Jena
Germany

Summary

The V3 loop of the HIV-1 envelope glycoprotein gp120 is involved in binding to the CCR5 and CXCR4 coreceptors. The structure of an HIV-1_{MN} V3 peptide bound to the Fv of the broadly neutralizing human monoclonal antibody 447-52D was solved by NMR and found to be a β hairpin. This structure of $V3_{MN}$ was found to have conformation and sequence similarities to β hairpins in CD8 and CCR5 ligands MIP-1α, MIP-1β, and RANTES and differed from the β hairpin of a $V3_{IIIB}$ peptide bound to the strain-specific murine anti-$gp120_{IIIB}$ antibody 0.5β. In contrast to the structure of the bound $V3_{MN}$ peptide, the $V3_{IIIB}$ peptide resembles a β hairpin in SDF-1, a CXCR4 ligand. These data suggest that the 447-52D-bound $V3_{MN}$ and the 0.5β-bound $V3_{IIIB}$ structures represent alternative V3 conformations responsible for selective interactions with CCR5 and CXCR4, respectively.

Introduction

The binding of the human immunodeficiency virus type-1 (HIV-1) to its target cells is mediated primarily by the envelope glycoprotein (gp120) of the virus. Binding of gp120 to CD4, a molecule found on the surface of both T cells and macrophages, triggers conformational changes in gp120 that expose a binding site to either CCR5 or CXCR4 chemokine receptors. Only after binding to the chemokine receptors can the virus penetrate into the target cell. The third hypervariable region of gp120 (V3 loop, residues 303–340) is directly involved in the binding to the chemokine receptors [1, 2]. The V3 sequence determines whether the virus binds to CCR5 (designated R5 virus) and, therefore, infects macrophages or whether it binds to CXCR4 (designated the X4 virus) and infects T cells ([3] and the references therein). A single mutation in the V3 loop, D329R, transformed an R5 virus into an X4 virus. A double mutation, S313R and D329Q or D333N, caused the same phenotype conversion [4]. (Residues are numbered throughout according to the BH10 isolate sequence [5]). Thus, small changes in the V3 sequence are sufficient to switch receptor selectivity of the virus.

Many HIV-1-neutralizing antibodies in infected individuals or in immunized animals are directed against the V3 loop, which was accordingly designated the principal neutralizing determinant (PND) of HIV-1 [6]. HIV-neutralizing antibodies against V3 are thought to prevent the binding of gp120 to either the CCR5 or CXCR4 chemokine receptor, thus abolishing fusion of the virus with its target cell [1, 2].

The structure of the gp120 core of both an X4 laboratory-adapted virus and that of an R5 primary isolate in complex with a CD4 fragment and the Fab of a gp120-specific antibody have been solved [7, 8]. However, crystals could be obtained only for gp120 lacking the first three variable loops, including V3, and the structures of V4 and V5 have not been defined. Despite the dramatic antigenic differences between the laboratory-adapted X4 and the primary R5 isolates, the structures of their gp120 cores are very similar [7]. These data, together with chimeric substitution and sequence analysis, indicate that coreceptor choice and neutralization resistance involve the major variable loops, V1/V2 and V3.

As an alternative to studying the V3 conformation in the intact gp120 molecule, complexes of V3 peptides with antibodies elicited against gp120 or HIV-1 can be used. Wilson and coworkers determined the crystal structures of $V3_{MN}$ peptides bound to three murine monoclonal antibodies generated against a cyclic 40-residue V3 peptide comprising the entire V3 loop [9–11]. An extended conformation and multiple turn conformations were observed, respectively, for the N- and C-terminal segments of the V3 loop flanking the central GPGR sequence. The GPGR segment itself was found to adopt dual conformations. However, the short epitopes recognized by these anti-peptide antibodies did not permit the determination of the global conformation of the $V3_{MN}$ loop. A strain-specific HIV-1-neutralizing murine monoclonal antibody, 0.5β, raised against $gp120_{IIIB}$, recognizes a significantly longer epitope in a $V3_{IIIB}$ peptide. The peptide bound to this antibody formed a β hairpin not observed in the X-ray studies [12]. The HIV-1_{IIIB} strain contains a QR insertion near the tip of the V3 loop present in less than 10% of HIV-1 isolates. This insertion is not found in the MN strain, which is a representative of the subtype B viruses common in Europe and North America [13].

The human monoclonal antibody 447-52D is one of the most broadly neutralizing and most potent anti-V3 antibodies that have been studied to date. It binds to intact virions from clades A, B, D, F, G, and H [14] and neutralizes primary isolates from several clades, includ-

*Correspondence: jacob.anglister@weizmann.ac.il

Key words: gp120 V3; NMR structure; HIV-1; coreceptor; neutralizing antibodies; chemokines

ing X4 and R5 viruses [15–20]. Antibody 447-52D binds to different V3 peptides with association constants of 2×10^5–10^8 M^{-1}, the highest of which is only one order of magnitude lower than its affinity to the corresponding gp120 protein [21]. Since 447-52D was elicited during the course of HIV-1 infection and neutralizes a broad spectrum of HIV-1 isolates, it most likely recognizes a native V3 conformation. Consequently, the structure of 447-52D complexed with V3 peptides can serve as a reliable model for understanding the interactions between gp120 and anti-HIV antibodies directed against V3 and for identifying features on the surface of the V3 loop that interact with the chemokine receptors on the target cells.

Here, we present the structure of a $V3_{MN}$ peptide (^{308}YNKRKRIHI—GPGRAFYTTKNIIG^{332}, where "—" represents the position of a two-residue insertion in $V3_{IIIB}$) as recognized by the Fv fragment of the HIV-1-neutralizing human monoclonal antibody 447-52D (447 Fv). The backbone of the bound peptide forms a β hairpin with two antiparallel β strands linked by an inverse γ turn. The N-terminal β strand and four residues from the C-terminal β strand contribute almost all the interactions between the V3 loop and the 447 Fv, indicating the exposure of these residues and, thereby, their potential to be involved in chemokine receptor binding. The V3 β hairpin shows conformation and sequence similarity to a β hairpin in CD8 and to β hairpins in MIP-1α, MIP-1β, and RANTES, which are implicated in binding to CCR5. The β hairpin conformation of a $V3_{IIIB}$ peptide bound to 0.5β-Fv is different and is shown to resemble a β hairpin in SDF-1, a CXCR4 ligand. This data suggests that these two β hairpin conformations of the V3 loop are responsible for coreceptor selectivity.

Results

Mapping the $V3_{MN}$ Epitope

NMR dynamic filtering was used to map the epitope within the $V3_{MN}$ peptide recognized by the 447 Fv. Peptide protons that do not interact with the Fv retain considerable mobility in comparison with peptide protons that interact with the Fv. As a result of the long mixing period used in the HOHAHA and ROESY spectra, the crosspeaks of peptide protons interacting with the Fv as well as of most Fv protons vanish, while the crosspeaks of residues in the flexible parts of the peptide that do not interact with the Fv are still observed. These include seven residues of the C-terminal region (^{MN}T326–^{MN}G332) and two of the N-terminal segment (^{MN}N309 and ^{MN}R311). The proton chemical shifts of these residues were practically identical to those observed for the free peptide, confirming that they do not interact or have only very minor interactions with the antibody. The HOHAHA crosspeaks of ^{MN}K312–^{MN}R322 were undetectable in the spectra, implying strong interactions with 447 Fv. The crosspeaks of ^{MN}A323, ^{MN}F324, and ^{MN}Y325 were weak, indicating that these three residues are within the $V3_{MN}$ epitope. By this method, the epitope recognized by the 447 Fv was mapped to gp120 residues ^{MN}K312–^{MN}Y325. This definition of the epitope was confirmed by examination of the peak intensity in a TROSY ^{1}H-^{15}N HSQC spectrum (Figure 1A) and by measurement of an HOHAHA spectrum of a ^{15}N-labeled peptide in complex with unlabeled Fv, which eliminated all interference by the Fv resonances (data not shown). Short ^{15}N T_2 relaxation times were measured for ^{MN}R311–^{MN}K328, indicating that some backbone immobilization of four additional residues, ^{MN}R311, ^{MN}T326, ^{MN}T327, and ^{MN}K328 (Figure 1B), occurs because of their proximity to the epitope and minor interactions with the 447 Fv (see below).

Solution Structure of the Antibody-Bound $V3_{MN}$ Peptide

The structure of the bound $V3_{MN}$ epitope was determined with 305 NMR-derived distance (90 long- and medium-range), 10 dihedral angle, and 2 hydrogen bond constraints. The superposition of the 29 lowest-energy structures that satisfy the experimental restraints with no NOE violations larger than 0.5 Å and no torsion angle violations exceeding 5° is shown in Figure 2A. The overall structure of the epitope ($^{312–327}$gp120) is well defined, with root-mean-square deviation (rmsd) values of 0.37 Å and 1.17 Å for the backbone and heavy atoms, respectively. The structural statistics and rmsd values are presented in Table 1. The Ramachandran plot (data not shown) of the mean structure of the complex suggests that the φ and ψ angles of the structure predominantly occupy allowed regions, except for ^{MN}G319 and ^{MN}G321.

As shown in Figures 2A–2C, the epitope forms a β hairpin consisting of two antiparallel β strands formed by residues ^{MN}R313–^{MN}I316 and ^{MN}A323–^{MN}T326 linked by a reverse turn. NOE interactions characteristic of a β hairpin conformation were observed between backbone atoms of the N-terminal and C-terminal halves. These interactions include ^{MN}R313 H^N/^{MN}T326 H^N, ^{MN}R313 H^N/^{MN}T327 H^α, ^{MN}I314 H^α/^{MN}Y325 H^α, and ^{MN}H315 H^N/^{MN}Y325 H^α. The expected ^{MN}K312 H^α/^{MN}T327 H^α and ^{MN}I314 H^α/^{MN}T326 H^N NOE interactions could not be assigned because of resonance overlap. $^3J_{HNH\alpha}$ coupling constants higher than 8.4 Hz, typical of a β strand, were measured for ^{MN}I314, ^{MN}H315, ^{MN}I316, ^{MN}Y325, ^{MN}T326, and ^{MN}T327.

In the NMR structure of the V3 epitope ($^{312–327}$gp120), the β hairpin is stabilized by a network of hydrogen bonds between the two β strands (Figure 2C). Two pairs of hydrogen bonds are formed between ^{MN}R313 and ^{MN}T326 and between ^{MN}H315 and ^{MN}F324. The side chains of residues ^{MN}R313, ^{MN}H315, ^{MN}F324, and ^{MN}T326 form the lower face of the β hairpin, while the side chains of ^{MN}I314, ^{MN}I316, ^{MN}A323, and ^{MN}Y325 form the upper face (Figure 2C). The structure of the β hairpin is stabilized by extensive hydrophobic interactions involving ^{MN}I314, ^{MN}I316, and ^{MN}Y325. The side chain of ^{MN}K312 forms additional stabilizing interactions with ^{MN}T327, ^{MN}I314, and ^{MN}Y325. On the lower face of the β sheet, only interactions between ^{MN}F324 and ^{MN}T326 could be observed, indicating that the lower face is less compact than the upper face. The precision and accuracy of the conformation of the side chains are expected to be improved when the structure of the entire Fv complex with the V3 peptide is solved. However, because of side chain interactions within the peptide, the conformation of some of the side chains is very well defined in the structure of the bound $V3_{MN}$ peptide. For example, the heavy-atom rmsd values for ^{MN}I314 and ^{MN}I316 are 0.175 and

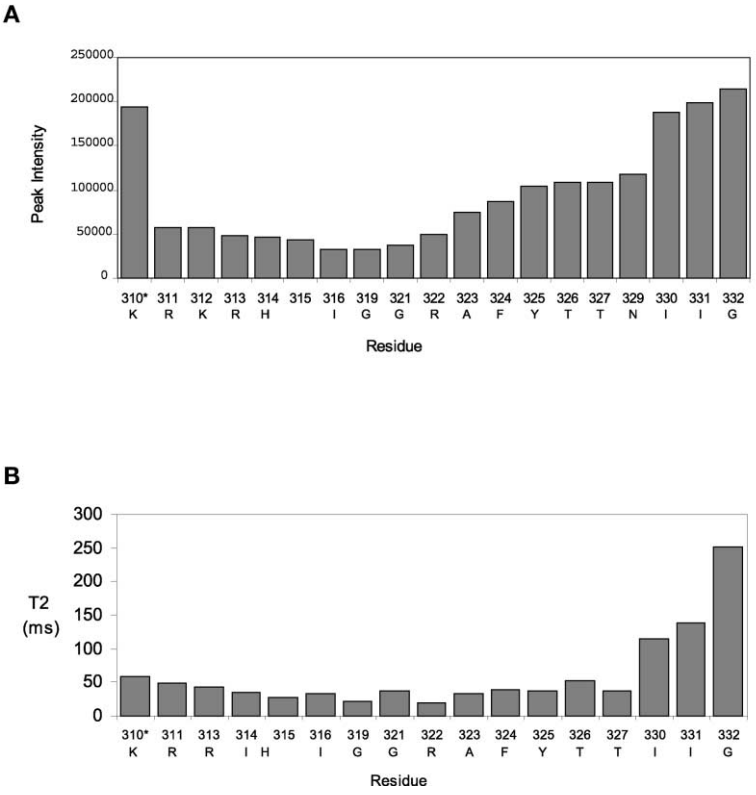

Figure 1. NMR Mapping of the 447-52D Epitope

(A) A diagram showing the variations in the $^{1}H^{N}/^{15}N$ crosspeak intensities of a ^{15}N TROSY-HSQC spectrum recorded with uniformly ^{15}N-labeled $V3_{MN}$ peptide bound to unlabeled 447 Fv.

(B) A diagram showing the variations of the ^{15}N T_2 relaxation times of the bound $V3_{MN}$ peptide along the peptide sequence. The asterisk denotes an overlap between residues ^{MN}K310 and ^{MN}K328.

0.361 Å, respectively, for the best backbone superposition of residues ^{MN}K312–^{MN}T327.

The GPG Segment Bound to 447 Fv Forms an Inverse γ Turn

The GPG sequence linking the β strands forms an inverse γ turn stabilized by an *i*,*i*+ 2 hydrogen bond between the carbonyl oxygen of ^{MN}G319 and the amide proton of ^{MN}G321. This γ turn conformation is corroborated by the sequential H^{δ}-H^{α} and H^{δ}-H^{N} connectivities between ^{MN}P320 and ^{MN}G319 (typical of proline in a *trans*-conformation), an NOE between ^{MN}P320 H^{α} and ^{MN}R322 H^{N}, and a strong sequential interaction between ^{MN}G321 H^{N} and ^{MN}P320 H^{α}. The φ and ψ angles of ^{MN}P320 are −72° and 65°, in excellent agreement with the characteristic inverse γ turn angles [22]. These differ markedly from the φ and ψ angles for a type II β turn (−60° and 120°) and a type I β turn (−60° and −30°). The side chain of ^{MN}R322 interacts extensively with the ^{MN}P320 and ^{MN}G319 residues that form the inverse γ turn, thus defining the orientation of the arginine side chain with respect to the turn (rmsd of 0.74 Å for the best backbone superposition of ^{MN}K312–^{MN}T327).

The $V3_{MN}$ Residues Interacting with the Antibody

Extensive interactions between the peptide and the 447 Fv were observed in the ^{13}C-edited NOESY spectrum. As shown in Figure 3, the N-terminal segment ^{MN}K312–^{MN}I316 contributes 59% of the peptide interactions with the Fv, with ^{MN}I316 contributing the largest number of interactions. The C-terminal segment comprising residues ^{MN}R322–^{MN}T327 contributes 33% of the interactions of the peptide with the Fv, significantly less than the N-terminal segment. The dominance of the N-terminal segment and ^{MN}R322 in the interactions with the 447 Fv (68% of the interactions with the 447 Fv) is supported by the dynamic-filtering experiments, which showed that the segment ^{MN}K312–^{MN}R322 was strongly immobilized upon binding to the 447 Fv. ^{MN}T326 and ^{MN}T327 have one interaction each with the Fv. The T_2 relaxation times of ^{MN}T326 and ^{MN}T327 are comparable to those of peptide residues that interact more extensively with the Fv, most likely because of interactions between the two β strands in the β hairpin involving these two residues (see above).

About half (55 out of 120) of the observed peptide side chain interactions with the Fv are with aromatic rings, indicating that the antibody binding site is rich in aromatic residues, as can be deduced from the sequence of the variable loops [23]. The existence of this aromatic environment is also reflected in the unusual high-field chemical shift observed for the protons of ^{MN}G319, ^{MN}P320, and ^{MN}R322 caused by the local ring current fields induced by aromatic amino acid residues [24]. As the antibody resonances have not yet been assigned, the peptide-Fv interactions could not be assigned to the specific 447 Fv residues involved.

The amide protons of ^{MN}I314 and ^{MN}I316 were found to exchange slowly with the solvent and were detected even 24 hr after exchanging H_2O with D_2O. All other amide protons disappeared because of fast exchange. This slow exchange of ^{MN}I314 and ^{MN}I316 amide protons indicated that they are protected from exchange with the solvent because of hydrogen bonds formed in the complex. As these two residues are not involved in hydrogen bonding within the β hairpin, they must be in-

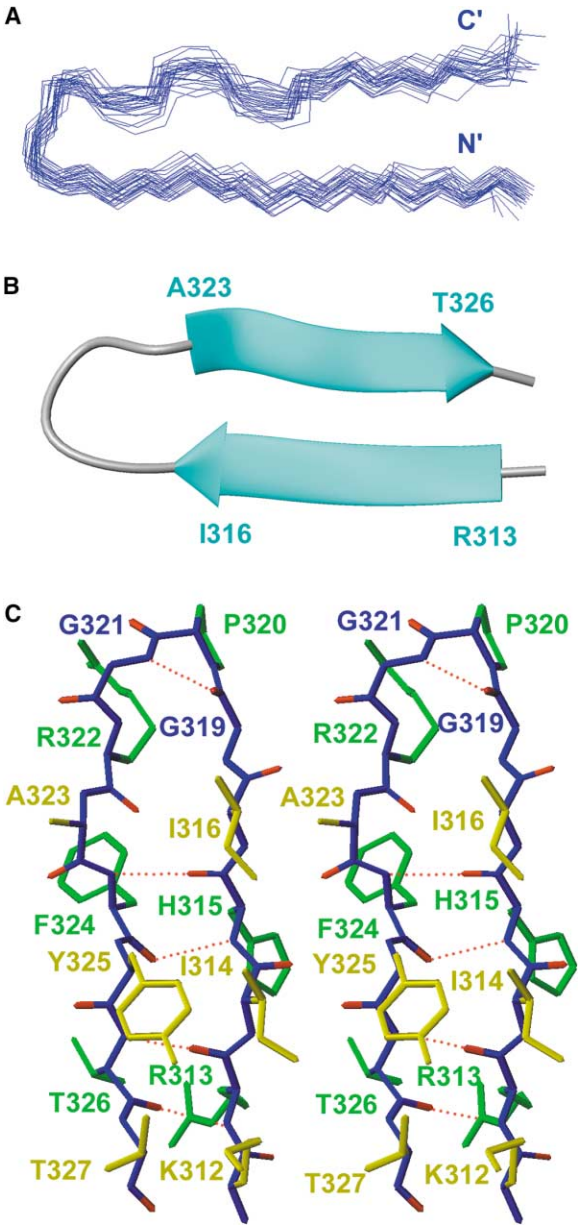

Figure 2. The Solution Structure of the $V3_{MN}$ Epitope ($^{312-327}gp120_{MN}$) Bound to the 447 Fv

(A) Backbone superposition of 29 lowest-energy structures.
(B) A ribbon diagram of the energy-minimized average structure; the terminal residues of the β strands are numbered.
(C) A stereo representation of $V3_{MN}$ bound to the 447 Fv showing side chain interactions and hydrogen bonds within the peptide (red). Side chains pointing out from the page, yellow; side chains pointing inward, green.

volved in intermolecular bonds to the Fv. The slow exchange of the amide protons indicates a very tight binding of the $V3_{MN}$ peptide to the 447 Fv.

The Structure of $V3_{MN}$ Bound to the 447 Fv Is Highly Homologous to β Hairpins in CD8, MIP-1α, MIP-1β, and RANTES

In an attempt to reveal potential structural homologs for the V3 β hairpin, we searched the Protein Data Bank using the SPASM program [25]. We found that, out of 9848 β hairpins that differed from the $V3_{MN}$ β hairpin by a backbone rmsd of less than 2.5 Å, 512 contained the motif IxI or homologs thereof, with conservative replacement of isoleucine by leucine or valine. Out of the six V3 residues found in this study to interact most extensively with the 447 Fv, ^{MN}I314, ^{MN}I316, and ^{MN}R322 are the most conserved, with 94%, 82%, and 91% conservation, respectively [26]. Of the 512 β hairpins, 54 and 60 had arginine or lysine separated by two or three residues, respectively, from the IxI motif or its homologs (conservative replacement of the isoleucine). In $V3_{MN}$, the two isoleucine residues are separated by histidine, which interacts extensively with the antibody but is conserved in only 46% of HIV-1 isolates [26]. In a search in which the "x" in the IxI motif was restricted to an aromatic residue, but not tryptophan, 10 β hairpins were found to have the (I/L/V) (H/F/Y) (I/L/V) x x x (R/K) motif. Three of these were human proteins; two were CD8 [27, 28] (in free and complexed form), and the third was an Alzheimer precursor protein [29]. As shown in Figure 4A the orientations of the two isoleucine residues and the positively charged side chain (K56 in CD8 and ^{MN}R322 in V3) are very similar in $V3_{MN}$ and CD8. The alignment of CD8 and $V3_{MN}$ sequences is presented in Figure 4D.

The search revealed that only seven of the homologous β hairpins had the sequence (I/L/V) (H/F/Y) (I/L/V) x x (R/K). The four that were of human origin included MIP-1α [30], RANTES [31], Met-RANTES [32], and an oncogene product involved in T cell prolymphocytic leukemia [33]. The sequence alignments of the MIP-1α and RANTES chemokines with the $V3_{MN}$ peptide are shown in Figure 4D. Of the three nonhuman β hairpins, one was a synthetic anti-HIV protein [34] and the other was a viral macrophage inflammatory protein-II (v-MIP) [35]. Five out of the seven peptides bind to CCR5. Although, according to the homology search, the basic amino acid in RANTES and MIP-1α is separated by two residues from the (I/L/V) (H/F/Y) (I/L/V) motif and by three residues in $V3_{MN}$, the side chain of the basic residue points in the same direction in the three proteins, and the overall topology of the (I/L/V) (H/F/Y) (I/L/V) sequence is similar, as shown in Figure 4B (H is neutral and aromatic at pH above the imidazole pKa). To test the uniqueness of

Table 1. NMR Constraints and Structural Statistics for the Refined 447 Fv-Bound V3MN Peptide (29 Structures)

NMR distance constraints	
Total	305
Intraresidue	155
Sequential	60
Medium- and long-range	90
Dihedral angle	10
NOE violations	
Maximum individual violation (Å)	0.5
Rmsd of NOE violation	0.0012 ± 0.0026
Deviation from ideal covalent geometry	
Bond lengths (Å)	0.0015 ± 0.0002
Bond angles (°)	0.4109 ± 0.0105
Improper angles	0.1394 ± 0.0183
Mean rmsd values (Å)	
All backbone atoms	0.37
All heavy atoms	1.17

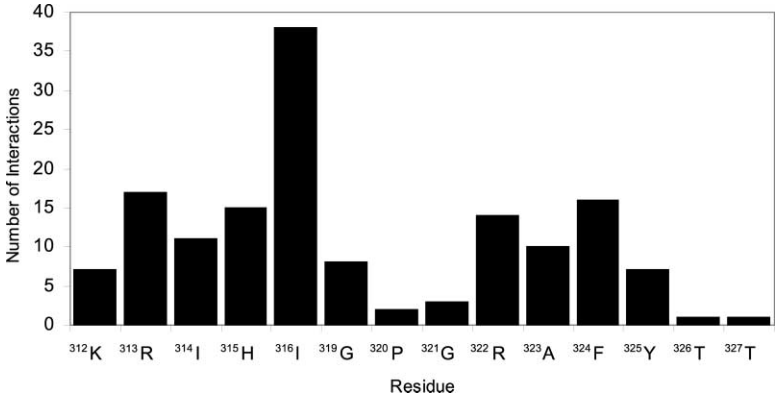

Figure 3. Intermolecular Interactions of the $V3_{MN}$ Peptide with the 447 Fv

The total number of intermolecular interactions observed in the NOESY spectra is shown for each residue of the epitope.

the similarity between $V3_{MN}$ and the corresponding β hairpins in MIP-1α and RANTES, we repeated the search for homologous β hairpins with a sequence (I/L/V) (H/F/Y) (I/L/V) x x x (R/K). Only human MIP-1α and RANTES and two rat proteins were revealed by the search, showing that the results are almost the same whether or not the positively charged residue is separated from the triad motif by two or four residues.

As shown in Figure 4D in MIP-1β, the residue following the aromatic residue is glutamine, instead of a nonpolar aliphatic amino acid; however, the remaining three residues of the motifs mentioned above are conserved [(I/L/V) (H/F/Y) x x x (R/K) and (I/L/V) (H/F/Y) x x x x x (R/K)]. The side chains of MIP-1β V41, F42, Q43, and R46 superimpose on the side chains of the corresponding residues ^{MN}I314, ^{MN}H315, ^{MN}I316, and ^{MN}R322 in $V3_{MN}$. The backbone rmsd between MIP-1β and the structure of $V3_{MN}$ bound to 447-52D is 1.88 Å for the segment IHIGPGRAFY, revealing the same structural homology between $V3_{MN}$ and MIP-1β as that observed between $V3_{MN}$ and MIP-1α and RANTES.

The $V3_{IIIB}$ Structure Recognized by 0.5β Fv Is Homologous to a β Hairpin in SDF-1

The IIIB strain has an atypical two-residue insertion at positions ^{IIIB}Q317 and ^{IIIB}R318 of the V3 loop. This insertion does not affect the length of the β strands in $V3_{IIIB}$ bound to 0.5β Fv in comparison with $V3_{MN}$ bound to 447-52D Fv but, rather, creates a six-residue loop comprising residues ^{IIIB}Q317, ^{IIIB}R318, ^{IIIB}G319, ^{IIIB}P320, ^{IIIB}G321, and ^{IIIB}R322, instead of the three-residue GPG loop in $V3_{MN}$ [12]. The reverse turn in $V3_{IIIB}$ is shifted one residue upstream and comprises the segment RGPG to maintain the central location of the reverse turn at the tip of the β hairpin. Therefore, to accommodate the two-residue insertion, the coordinates for ^{IIIB}G319 and ^{IIIB}P320 at the tip of the turn were excluded when the SPASM program was used to search the Protein Data Bank for structural homologs of the $V3_{IIIB}$ β hairpin. We found that, out of 5734 β hairpins that differed from the $V3_{IIIB}$ β hairpin by a backbone rmsd of less than 1.0 Å, only the structure of SDF-1 [36, 37] in the Protein Data Bank contained the (I/L/V/A) (H/R/K) (I/L/V/A) motif (H is included, since it is positively charged at pH below the imidazole pKa). The backbone superposition of the SDF-1 β hairpin over the $V3_{IIIB}$ β hairpin (Figure 4C) shows an excellent fit, with a backbone rmsd of 0.47 Å when the segments KSIRIQR and RAFVTI of $V3_{IIIB}$ are superimposed over the segments IVARLKN and NRQVCI of SDF-1 (see Figure 4D). Interestingly, residues ^{IIIB}G319 and ^{IIIB}P320 at the tip of the turn protrude beyond the common structure as a result of the longer loop. SDF-1 has an arginine residue after the reverse turn, as does $V3_{IIIB}$, but this arginine is shifted one residue downstream in the SDF-1 sequence.

Discussion

The Neutralizing Face of the V3 Loop

In this study, the structure of a 23-residue $HIV\text{-}1_{MN}$ V3 peptide bound to the Fv fragment of the human monoclonal antibody 447-52D in solution was solved by multidimensional heteronuclear NMR, and the interactions between the peptide and 447 Fv were assigned to specific peptide residues. The V3 epitope ($^{312–327}$gp120) bound to 447 Fv forms a β hairpin consisting of two antiparallel β strands comprising residues ^{MN}R313–^{MN}I316 and ^{MN}A323–^{MN}T326 linked by an inverse GPG γ turn (Figure 2C). Residues ^{MN}K312, ^{MN}R313, ^{MN}I314, ^{MN}H315, and ^{MN}I316 from the N-terminal strand and residues ^{MN}R322, ^{MN}A323, ^{MN}F324, and ^{MN}Y325 from the C-terminal strand form most of the intermolecular interactions of the $V3_{MN}$ peptide with the 447 Fv (Figure 3). These residues form an exposed surface of the V3 loop that has the potential to interact with the chemokine receptors CCR5 and CXCR4. Indeed, alanine scanning showed that V3 residues ^{MN}K312, ^{MN}I314, ^{MN}R322, and ^{MN}F324 are important for CCR5 binding [38]. Moreover, each of these residues is highly conserved: ^{MN}I314 is found in 94% of HIV-1 isolates, ^{MN}K312 and ^{MN}R322 are identical or conservatively replaced by arginine or lysine, respectively, in 95% and 91.5% of HIV-1 isolates, and ^{MN}F324 is conserved in 71% of HIV-1 isolates [26].

Previously we showed that, in the complex of a $V3_{IIIB}$ peptide bound to the strain-specific HIV-1-neutralizing murine monoclonal antibody 0.5β, residues ^{IIIB}I314, ^{IIIB}R315, ^{IIIB}Q317, ^{IIIB}P320, ^{IIIB}R322, and ^{IIIB}F324 form most of the interactions with the antibody [39]. Thus, the NMR studies to date indicate that the N-terminal segment close to the tip of the V3 loop and, to a lesser extent, the C-terminal segment following the GPG sequence are recognized by HIV-1-neutralizing anti-V3 antibodies.

The crystal structure of $V3_{MN}$ peptides in complex with three murine monoclonal antibodies, 50.1, 59.1, and 58.2, elicited against a cyclic peptide comprising the

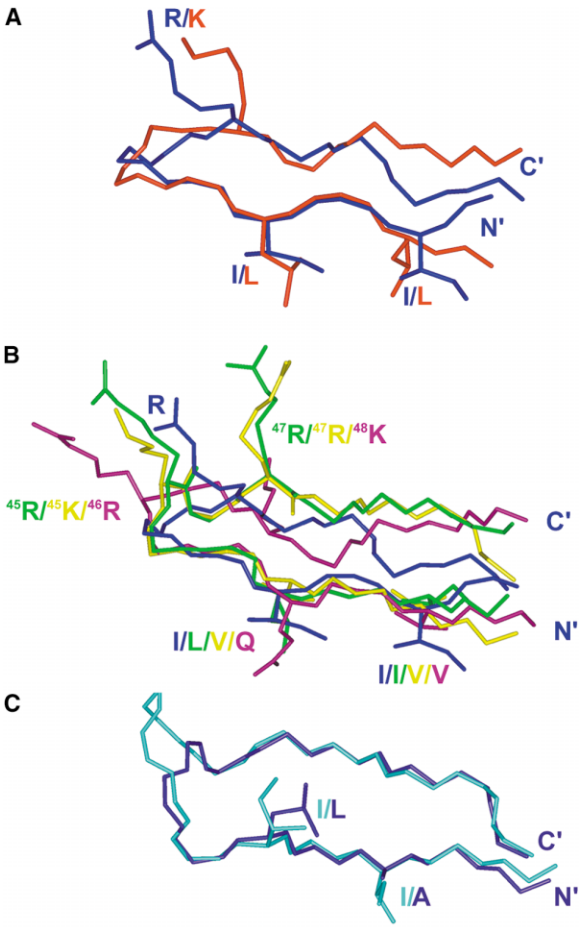

D

$V3_{MN}$	$-^{312}$KRIHIGPGRAFYTT^{327}
CD8	$-^{48}$FLLYLSQNKPKAAE^{61}
MIP-1α	$-^{38}$GVIFLTKRSRQVCA^{51}
MIP-1β	$-^{39}$AVVFQTKRSKQVCA^{52}
RANTES	$-^{38}$AVVFVTRKNRQVCA^{51}
$V3_{IIIB}$	$-^{312}$KSIRIQRGPGRAFVTI^{327}
SDF-1	$-^{38}$IVARLKN--NNRQVCI^{51}

Figure 4. Structural Homology of the V3 β Hairpins with CD8, MIP-1α, MIP-1β, RANTES, and SDF-1

Backbone superposition of the 447 Fv-bound $V3_{MN}$ peptide (blue) with (A) CD8 (red) and (B) CCR5 natural ligands MIP-1α (green), MIP-1β (magenta), and RANTES (yellow). The side chains of I314, I316, and R322 in $V3_{MN}$ and their equivalents in CD8 (L50, L52, and K56), MIP-1α (I40, L42, R45, or R47), MIP-1β (V41, Q43, R46, or K48) and RANTES (V40, V42, K45, or R47) are shown.

(C) Backbone superposition of the 0.5β Fv-bound $V3_{IIIB}$ peptide (cyan) with SDF-1 (purple). Side chains of I314 and I316 of $V3_{IIIB}$ and A40 and L42 in SDF-1 are shown.

(D) Sequence alignment of the V3 peptides with the homologous β hairpins in CD8, MIP-1α, MIP-1β, RANTES, and SDF-1.

entire V3 loop was solved by X-ray crystallography [9–11]. Antibody 50.1 interacts with ^{MN}K312–^{MN}P320, antibody 59.1 interacts with ^{MN}I316–^{MN}F324, and antibody 58.2 interacts with ^{MN}R313–^{MN}Y325. The combined epitope recognized by the three anti-peptide antibodies overlaps the epitope recognized by human monoclonal antibody 447-52D, excluding ^{MN}T326 and ^{MN}T327. While antibodies 59.1 and 58.2 showed no obvious preference for antibody interactions with the N-terminal strand of the epitope, antibody 50.1 interacts only with the N-terminal strand and the beginning of the turn.

The β Hairpin Is a Common Structural Feature of V3 Loops of Different HIV-1 Strains

Since antibody 447-52D was elicited against the HIV-1 virus, binds to intact virions [14], and neutralizes a broad spectrum of viruses [18], it recognizes a V3 conformation that exists on virus particles. Flexible V3 peptides, when bound to such an antibody, will assume the conformation against which this antibody was elicited. The antibody 0.5β, which we studied previously, was elicited against soluble gp120, and, therefore, this antibody also recognizes a V3 conformation in the context of the whole protein [12]. In contrast, the linear $V3_{MN}$ peptide and its cyclic form used as an immunogen in obtaining the three anti-peptide antibodies studied by crystallography are mostly flexible in the free form and, except for a β turn in the GPGR segment, they do not show any detectable secondary structure in aqueous solution [40].

We previously observed a β hairpin conformation with a type VI β turn in the $V3_{IIIB}$ peptide bound to 0.5β Fv [12]. Therefore, both our present and previous findings suggest that the β hairpin is conserved in the V3 region of gp120 from different virus strains. This conclusion is consistent with the prediction that the V3 loop of most HIV-1 strains forms a β strand, β turn, and β strand conformation [26, 41]. It is important to note that, while the X-ray structures agree with the secondary structure predictions with respect to the N-terminal segment, they either provide no information or have different structures (multiple turns) for the C-terminal residues [9–11].

The Flexibility of the GPGR Sequence

The GPGR segment was found to adopt different types of reverse turn when bound to different HIV-1 antibodies, as summarized in Figures 5A and 5B. The inverse γ turn observed in $V3_{MN}$ bound to the 447 Fv differs from the type II and type I β turns in the $V3_{MN}$ peptide bound to the anti-peptide antibodies and from the type VI cis-proline β turn that was observed in the RGPG segment at the center of a $V3_{IIIB}$ peptide bound to the 0.5β Fv [12]. The different types of turn suggest a conformational flexibility in the GPGR sequence, a flexibility that is likely conferred by the two glycine residues flanking the proline. As a result of this flexibility, the GPGR segment may adopt different conformations according to the sequence of the V3. Thus, it is possible that the rare QR insertion that precedes the GPGR segment in $V3_{IIIB}$ caused the shift in the β turn in order to preserve the alignment of the hydrogen bonds in the β hairpin [12]. This may conserve the spatial arrangement of the side chains crucial for binding to the chemokine receptors. In addition, conformational flexibility of the V3 loop may contribute to the topology of the β hairpin surface exposed to the HIV coreceptors and allow the V3 region to optimize its conformation to maximize its binding to one or more of the chemokine receptors (see below).

A

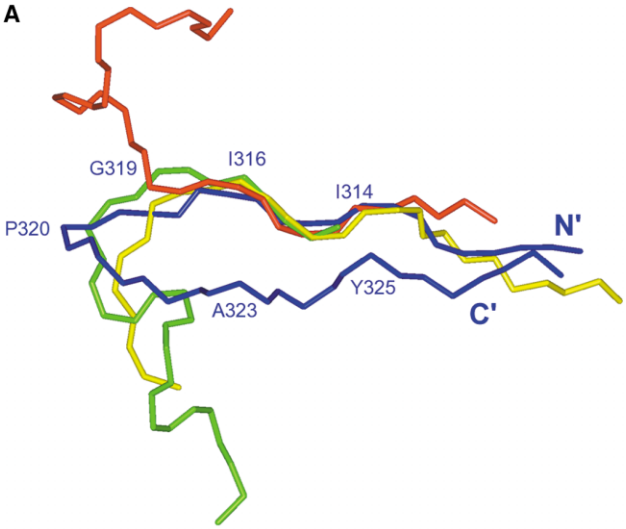

Figure 5. The Structure of the $V3_{MN}$ Peptide Bound to the 447 Fv Compared with the Structures of V3 Peptides Bound to Anti-Peptide Antibodies

(A) Backbone superposition of the bound $V3_{MN}$ peptides in complex with the 447 Fv (blue) or with antibodies 50.1 (yellow), 59.1 (green), and 58.2 (red).

(B) The epitope recognized by each antibody and the type of turn the bound peptide forms in each complex. Residues in β strands are underlined. The residues in bold letters form turns.

B

Antibody/peptide	Epitope & Structure turn	
447/$V3_{MN}$	KRIHI--**GPG**RAFYTT	inverse γ
0.5β/$V3_{IIIB}$	KSIRIQ**RGPG**RAFVTI	type VI β
50.1/$V3_{MN}$	KRIHI--**GPG**	type II β
59.1/$V3_{MN}$	HI--**GPGRAF**YT	type II- type I β
58.2/$V3_{MN}$	RIHI--**GPGRAFY**	type I- type I β

Alternative Conformations of the V3 Loop

Although both the $V3_{IIIB}$ peptide bound to 0.5β Fv and the $V3_{MN}$ peptide bound to 447 Fv form β hairpins, they differ in the network of hydrogen bonds within the two peptides that stabilize the β hairpin conformation. While, in the $V3_{IIIB}$ peptide, ^{IIIB}K312, ^{IIIB}I314, and ^{IIIB}I316 form hydrogen bonds with ^{IIIB}I327, ^{IIIB}V325, and ^{IIIB}A323, respectively, there is a one-residue shift in the intrapeptide hydrogen bonds in the $V3_{MN}$ peptide, where residues ^{MN}R313 and ^{MN}H315 form hydrogen bonds with residues ^{MN}T326 and ^{MN}F324, respectively. As a result of this shift, side chains pointing upward in $V3_{IIIB}$ point downward in $V3_{MN}$, as if the two conformations were related by an imaginary inversion axis. As shown in Figure 6A, superpositioning of the IHI segment of $V3_{MN}$ over the corresponding IRI segment in $V3_{IIIB}$ results in a 180° difference in the direction of the continuation of the β turn and the second β strand. In the context of the gp120 protein, residues exposed in one type of β hairpin may be buried in the other β hairpin conformation and vice versa. These differences in orientation may have profound implications on coreceptor and antibody binding.

Superpositioning of the IFL segment in MIP-1α, the VFV segment in RANTES, and the VFQ segment in MIP-1β over the ARL motif of SDF-1 created the same 180° rotation as that observed between $V3_{MN}$ and $V3_{IIIB}$ (Figure 6A). The effect of this change in conformation is illustrated in a comparison of MIP-1α and SDF-1 (Figures 6B and 6C). The ribbon diagrams (in red) show that the overall spatial orientation of the backbones of these chemokines is quite similar. Nevertheless, the space-filling blowup of the β hairpins clearly shows that, in MIP-1α, residue F41 is buried and residues I40 and L42 are exposed (Figure 6B). In SDF-1, a 180° flip results in the exposure of residue R41 and the burial of residues A40 and L42 (Figure 6C). It is evident that the topology of the side chains of these amino acid triads is inverted in these two chemokines.

The topology of the V3 loop with respect to native gp120 is unknown. Figures 6D and 6E show the orientation of $V3_{MN}$ and $V3_{IIIB}$ obtained by superpositioning them over the homologous β hairpins in MIP-1α and SDF-1, respectively. This superpositioning shows a remarkable resemblance in the orientation of the triad residues between $V3_{MN}$ (IHI) and MIP-1α (IFL) and between $V3_{IIIB}$ (IRI) and SDF-1 (ARL). As with MIP-1α and SDF-1, the orientation of the side chains of the $V3_{MN}$ triad IHI is inverted in comparison with the orientation of the side chains of the $V3_{IIIB}$ IRI triad (Figures 6D and 6E). Thus, the alternative conformations found in the $V3_{MN}$ and $V3_{IIIB}$ β hairpins are highly analogous to the alternative β hairpin conformations found in MIP-1α/MIP-1β/RANTES and SDF-1, respectively.

Varying conformations of the V3 loop around the GPGR β turn were previously observed by Wilson and coworkers when comparing three different anti-V3 peptide antibodies in complex with a $V3_{MN}$ peptide. However, the β hairpin conformation was not observed [11], thus preventing the observation of the one-residue shift in the hydrogen bond network and its implications on side chain orientation and surface topology.

The Homology between the V3 Loop and β Hairpin Structures of MIP-1α/MIP-1β/RANTES and SDF-1

The correlation between the conformation of $V3_{MN}$ bound to the 447 Fv and the β hairpins in MIP-1α, MIP-1β, and RANTES suggests that the conformation of V3 recognized by the 447 Fv may be the conformation interacting

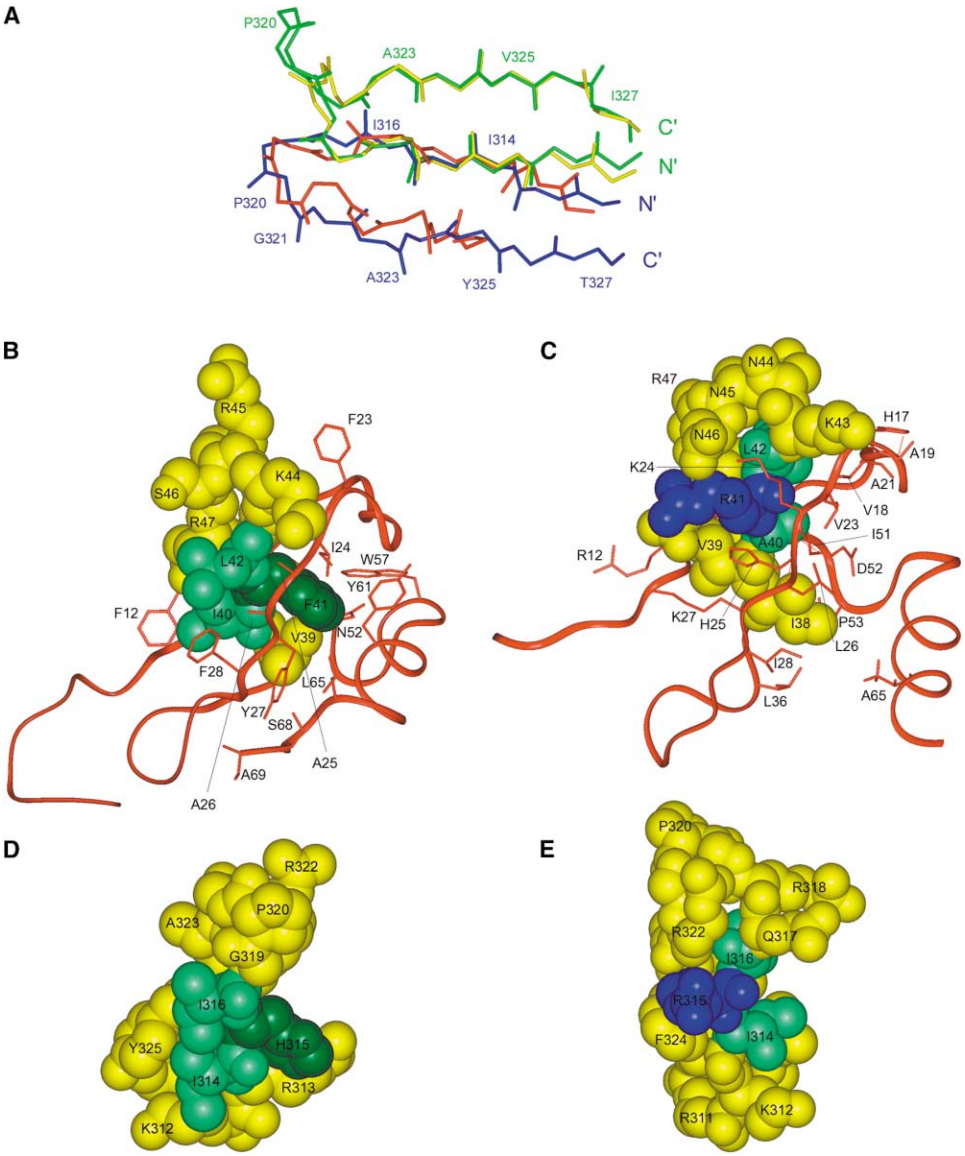

Figure 6. Analogy between the Dual β Hairpin Conformations Formed by V3 Loops and the Conformations of the Homologous β Hairpins in MIP-1α and SDF-1

(A) Backbone superposition of the homologous β hairpins in SDF-1 (yellow), $V3_{IIIB}$ (green), MIP-1α (red), and $V3_{MN}$ (blue) obtained by best superposition of triads I40-F41-L42 (MIP-1α), A40-R41-L42 (SDF-1), I314-H315-I316 ($V3_{MN}$), and I314-R315-I316 ($V3_{IIIB}$). A ribbon diagram of (B) MIP-1α and (C) SDF-1. The β hairpins homologous to V3 are shown in a space-filling view, while nearby residues are shown in sticks. (D) $V3_{MN}$ and (E) $V3_{IIIB}$ presented in a space-filling representation. The residues of the above triads are highlighted. Residues I40 and L42 in MIP-1α, A40 and L42 in SDF-1, and I314 and I316 in both $V3_{MN}$ and $V3_{IIIB}$ are light green. The aromatic residues F41 in MIP-1α and H315 in $V3_{MN}$ are dark green, and R41 in SDF-1 and R45 in MIP-1α are blue.

with CCR5. Thus, the VFV motif in RANTES is part of the β2 strand (residues 38–43), which forms a β sheet with the β1 strand of the protein. Both β strands are implicated in binding to CCR5 [42]. The corresponding region of the V3 loop also participates in chemokine binding [38]. The observation that affinity-purified anti-V3 antibodies isolated from HIV-1-infected patients crossreact with MIP-1α and RANTES [43] further supports the apparent homology between the structures of V3 and these chemokines. However, since the sequence identity between the 447-52D epitope and the corresponding region in MIP-1α is only 7%, it is unlikely that a monoclonal antibody such as 447-52D will crossreact with MIP-1α, MIP-1β, and RANTES. The correlation between the structure of $V3_{IIIB}$ bound to 0.5β and that of SDF-1 (Figure 6) also suggests that the conformation of bound $V3_{IIIB}$ represents that of the V3 loop in X4 HIV-1 viruses.

Further evidence supporting the proposed homology between V3 and the β hairpin structures of the chemokines, which are ligands for the HIV-1 coreceptors, is provided by experiments from several groups that have

shown that V3 loop-derived peptides can inhibit viral entry into target cells in a coreceptor-specific manner [44–46].

The Mechanism for Coreceptor Selectivity

Four residues implicated in CCR5 binding (K312, I314, R322, and F324) are contained in the V3 β hairpin [38] recognized by 447-52D. The orientation of each of these amino acids is reversed in the β hairpin conformations of bound $V3_{MN}$ and $V3_{IIIB}$, and it is difficult to envision how these alternative conformations could bind to the same receptor. If $V3_{MN}$ bound to 447 Fv is in an R5 virus conformation and the $V3_{IIIB}$ bound to 0.5β is in an X4 virus conformation, the differences in these critical residues could account for coreceptor selectivity.

As noted above, the overall spatial arrangements of the backbones of MIP-1α/MIP-1β/RANTES and SDF-1 show significant homology (Figures 6B and 6C), and common sequence motifs appear in both. Further analogies emerge upon inspection of their electrostatic properties. As seen in Figure 6C, the β1 strand adjacent to the ARL motif of SDF-1 contains positively charged residues K24, K27, and H25, which can be positively charged, depending on its pKa. In contrast, MIP-1α has I24, A25, and Y27 in the corresponding positions of the β1 strand (Figure 6B), creating a neutral and more-hydrophobic surface adjacent to the I40-F41-L42 triad in the three-dimensional structure of the protein. It is known that an increased positive charge at the base of the V3 loop transforms an R5 virus into an X4 virus. Residue 329 is very important for coreceptor selectivity. It is two residues downstream of the β hairpin C terminus, and mutation from D to R results in a switch from an R5 to an X4 isolate [4]. It is possible that placing a positively charged residue at this position in V3 results in a change in the charge of the surface that mimics the positively charged β1 strand in SDF-1 (see above). If this is correct, it suggests that an increased positive charge and a β hairpin conformation that mimics the SDF-1 surface are involved in CXCR4 binding, while a less positive surface and an MIP-1α-like β hairpin conformation mimic the MIP-1α, MIP-1β, and RANTES surface involved in CCR5 binding.

As stated earlier, the 447-52D antibody was elicited in an HIV-1-infected individual, and, therefore, the exact strain and V3 sequence responsible for its production are unknown. Antibody 447-52D neutralizes a broad spectrum of HIV-1 isolates from different clades, including primary X4 and R5 viruses. The epitope recognized by 447-52D does not include residue 329, which is the most crucial for coreceptor selectivity. Moreover, the consensus sequence of clade B R5 viruses in the region of the 447-52D epitope ($^{312–327}$gp120) differs by only one residue from the MN sequence (R313 is replaced by Ser in R5 viruses). Apparently this replacement does not interfere with 447-52D binding, since $V3_{IIIB}$ contains this replacement and $HIV\text{-}1_{IIIB}$ is neutralized by 447-52D [47]. The importance of residue 313 for coreceptor selectivity, but its minor effect, if any, on 447-52D binding, could be due to the fact that this residue is at the periphery of the 447-52D epitope.

Since V3 peptides are flexible and the V3 loop of X4 and R5 viruses may differ only slightly in the epitope recognized by an HIV-1-neutralizing antibody, the antibody can induce the peptide to adopt the conformation against which the antibody was elicited. In such a case, it would not matter whether the peptide used to obtain the complex is from an X4 or an R5 virus. This would explain why the $V3_{MN}$ peptide, which represents the V3 sequence of an X4 virus, binds to the 447 Fv in an R5 topology. Clearly, the proof for the involvement of such conformational changes in coreceptor selectivity will require determination of the structure of gp120, including V3 in complex with the chemokine receptors CXCR4 and CCR5. Nevertheless, our NMR structural studies of V3 loop peptides bound to HIV-1-neutralizing antibodies and structural comparisons with the natural ligands of the HIV-1 coreceptors provide compelling data that illuminate the mechanisms underlying coreceptor selectivity and bypass the difficulties in crystallizing membrane proteins, which preclude such experiments at this time.

However, it is not altogether clear how antibody 447-52D can neutralize both X4 and R5 viruses. One possible explanation is that there is equilibrium between the two β hairpin conformations of the V3 and that both are present under physiological conditions. The selection of the coreceptor is dictated mostly by residue 329 and, to a lesser extent, by the charges of residues 312 and 313. Since residue 329 is outside the epitope recognized by 447-52D, the antibody can neutralize X4 and R5 viruses, which have very similar sequences in the 447-52D epitope ($^{312–327}$gp120). V3 conformational flexibility could shift the equilibrium to the R5 conformation upon binding of the virus to 447-52D. Interestingly, an equilibrium between two β hairpin conformations differing in the pattern of hydrogen bonds was observed by NMR in the C chemokine lymphotactin [48], providing clear evidence for the feasibility of the V3 flexibility model. This dual conformation of the lymphotactin β hairpin was accompanied by a shift of one residue in the pattern of hydrogen bonds with a third β strand that forms a three-strand β sheet with the hairpin. Similar interactions between V3 and other regions of gp120 could play a role in the conformational equilibrium of V3.

Biological Implications

Our structural studies on anti-gp120 and anti-HIV-1 antibodies directed against V3 show that the V3 loop can assume two types of β hairpin, differing in the network of hydrogen bonds by a one-residue shift. As a result, the orientation of the V3 residues within gp120 and their exposure are very different for the two V3 conformations, even though the sequence at the central ten-residue segment of V3 is highly homologous. One type of β hairpin shows structural and sequence similarity to MIP-1α, MIP-1β, and RANTES β hairpin structures implicated in CCR5 binding, and the other V3 β hairpin conformation shows structural and sequence similarity to a β hairpin in SDF-1, a CXCR4 ligand. The data suggest a role for the dual V3 conformations in coreceptor selectivity.

Experimental Procedures

Sample Preparation

The $V3_{MN}$ peptide $^{308–332}gp120_{MN}$ (YNKRKRIHIGPGRAFYTTKNIIG) linked to a fusion protein was expressed in *Escherchia coli*, cleaved,

and purified as previously described [49] (note that the sequential numbering system in $V3_{MN}$ is interrupted because of a rare two-residue insertion in HIV-1_{IIIB}, and, therefore, residues 317 and 318 are not present in $V3_{MN}$). The 447 Fv was expressed in the BL21(DE3)-pLysS strain [50]. The Fv-peptide complex (28.7 kDa) was prepared by the addition of a 20% molar excess of the peptide to a dilute Fv solution ($\sim$0.04 mM). The sample was concentrated by membrane filtration with vivaspin (Vivascience) with a 10 kDa cut-off. All samples contained 10 mM sodium acetate buffer and 0.05% NaN_3 (pH 5).

NMR Spectroscopy

NMR spectra were acquired at 35°C on Bruker DMX 500 and DRX 800 spectrometers with unlabeled $^{308-332}gp120_{MN}$ or peptide uniformly labeled with ^{15}N or with ^{13}C and ^{15}N in complex with unlabeled 447 Fv. ROESY and HOHAHA spectra with long mixing times (90 ms) were used for epitope mapping. The mixing time was adjusted to discriminate between crosspeaks of peptide protons that are immobilized in the complex because of interactions with the antibody and that have a short $T_{1\rho}$ relaxation time and those of protons that do not interact with the Fv and, therefore, retain considerable mobility and have a long $T_{1\rho}$. Two-dimensional spectra of the unlabeled complex were measured at 30°C, 20°C, and 10°C and at pH 7, 5, and 4.25. The combination of the HOHAHA and ROESY spectra was used for sequential assignment of the mobile segments of the peptide in the Fv-peptide complex. A 2D ^{15}N-edited TOCSY of ^{15}N-labeled peptide in complex with unlabeled Fv was measured to confirm the definition of the epitope. T_2 ^{15}N relaxation time measurements [51] were carried out with a total of 182 transients. Six time points were collected with parametric delays of 8, 16, 24, 32, 48, and 72 ms at 18.79 T, with a 2 s delay between scans.

Complete sequential and side chain assignment of ^1H, ^{13}C, and ^{15}N resonances of the bound peptide, including the epitope residues, was accomplished with TROSY-HNCA, CT-CBCA(CO)NH, TROSY-HNCACB, HBHA(CO)NH, HCCH-COSY, and HCCH-TOCSY experiments ([52] and the references therein). The assignment of the aromatic side chains was done with 2D ^{13}C-TROSY ([53] and the references therein).

Distance constraints were derived from two 3D ^{13}C-edited NOESY spectra, one optimized for the aliphatic protons and the other optimized for the aromatic protons (80 ms mixing time in D_2O), and a ^{15}N-edited TROSY-NOESY in H_2O (75 ms mixing time) [53]. Slowly exchanging amide protons were identified by recording a series of 2D ^{15}N TROSY-HSQC spectra immediately after the H_2O buffer was exchanged with D_2O buffer. The 3D ^{15}N- and ^{13}C-separated NOESY spectra acquired with a $^{13}C/^{15}N$-labeled $V3_{MN}$ peptide, $^{308-332}gp120_{MN}$, in complex with the unlabeled 447 Fv, revealed inter- and intramolecular peptide NOEs.

φ angle restraints were determined from $^3J_{HNH\alpha}$ coupling constants, obtained from a 3D HNHA spectrum [54]. The values of $^3J_{HNH\alpha}$ determined from peak intensity ratio were scaled by a factor of 1.2 to account for fast spin-flips during the dephasing period. The φ angles of residues with $^3J_{HNH\alpha}$ values smaller than 6 Hz and larger than 8.4 Hz were constrained to $-65° \pm 25°$ and $-120° \pm 30°$, respectively. $^3J_{HNH\alpha}$ values between 6 and 8 Hz were considered as uninformative [55]. Three ψ angles for residues ^{MN}I314, ^{MN}H315, and ^{MN}I316 were included in the calculations on the basis of analyses of predictions from the TALOS [56] program with chemical shifts of ^1H, $^{13}C\alpha$, $^{13}C\beta$, and ^{15}N. NMR spectra were processed with NMRpipe/NMRDraw [57] or with Bruker's XWINNMR software and analyzed with AURELIA [58].

Structure Calculations

Interproton distance restraints were obtained from peak intensities. For each NOE involving a methyl group 0.5 Å was added, and 1 Å was added for constraints involving methyl-methyl interaction. The upper bound distance constraints were 130% of the NOE-derived distances to account for internal motion and proton multiplicity [55], and the lower bound distance was set to 1.8 Å. Structure calculations were performed with CNS 1.1 [59] and a dynamic simulated-annealing protocol starting with extended initial structures. The ambiguous NOEs were assigned in an iterative manner with structures calculated on the basis of the already assigned NOEs. Two hydrogen bonds were used as restraints in later stages of refinement on the basis of characteristic backbone NOEs between two anti-parallel β strands. Secondary structure elements and rmsd values were calculated with the MOLMOL program 2.6 [60]. Structures were further analyzed with Aqua/Procheck-NMR [61] and displayed with InsightII (MSI).

Acknowledgments

We thank Professor Fred Naider for illuminating discussions and for careful editing of the manuscript, Mr. Yehezkiel Haik for peptide purification, Dr. Anat Zvi for cloning and sequencing 447-52D, Mrs. Min-Ji for expressing 447 Fv in *E. Coli* and developing the purification protocol, Mr. Ran Lati for Fv production, Dr. Vitali Tugarinov, Mr. Jordan Chill, and Dr. Tali Scherf for help in the NMR experiments, and Dr. Mirek Gorny for the immunological characterization of 447-52D and helpful discussions. This study was supported by the Minerva Foundation, Germany (J.A.), and by NIH grants GM 53329 (J.A.), AI 36085 (S.Z.P.), and HL 59725 (S.Z.P.). J.A. is the Dr. Joseph and Ruth Owades Professor of Chemistry.

Received: August 16, 2002
Revised: December 26, 2002
Accepted: January 2, 2003

References

1. Trkola, A., Dragic, T., Arthos, J., Binley, J.M., Olson, W.C., Allaway, G.P., Cheng-Mayer, C., Robinson, J., Maddon, P.J., and Moore, J.P. (1996). CD4-dependent, antibody-sensitive interactions between HIV-1 and its co-receptor CCR-5. Nature *384*, 184–187.
2. Wu, L., Gerard, N.P., Wyatt, R., Choe, H., Parolin, C., Ruffing, N., Borsetti, A., Cardoso, A.A., Desjardin, E., Newman, W., et al. (1996). CD4-induced interaction of primary HIV-1 gp120 glycoproteins with the chemokine receptor CCR-5. Nature *384*, 179–183.
3. Moore, J.P., Trkola, A., and Dragic, T. (1997). Co-receptors for HIV-1 entry. Curr. Opin. Immunol. *9*, 551–562.
4. De Jong, J.J., De Ronde, A., Keulen, W., Tersmette, M., and Goudsmit, J. (1992). Minimal requirements for the human immunodeficiency virus type 1 V3 domain to support the syncytium-inducing phenotype: analysis by single amino acid substitution. J. Virol. *66*, 6777–6780.
5. Ratner, L., Haseltine, W., Patarca, R., Livak, K.J., Starcich, B., Josephs, S.F., Doran, E.R., Rafalski, J.A., Whitehorn, E.A., Baumeister, K., et al. (1985). Complete nucleotide sequence of the AIDS virus, HTLV-III. Nature *313*, 277–284.
6. Rusche, J.R., Javaherian, K., McDanal, C., Petro, J., Lynn, D.L., Grimaila, R., Langlois, A., Gallo, R.C., Arthur, L.O., Fischinger, P.J., et al. (1988). Antibodies that inhibit fusion of human immunodeficiency virus-infected cells bind a 24-amino acid sequence of the viral envelope, gp120. Proc. Natl. Acad. Sci. USA *85*, 3198–3202.
7. Kwong, P.D., Wyatt, R., Majeed, S., Robinson, J., Sweet, R.W., Sodroski, J., and Hendrickson, W.A. (2000). Structures of HIV-1 gp120 envelope glycoproteins from laboratory-adapted and primary isolates. Structure *8*, 1329–1339.
8. Kwong, P.D., Wyatt, R., Robinson, J., Sweet, R.W., Sodroski, J., and Hendrickson, W.A. (1998). Structure of an HIV gp120 envelope glycoprotein in complex with the CD4 receptor and a neutralizing human antibody. Nature *393*, 648–659.
9. Ghiara, J.B., Stura, E.A., Stanfield, R.L., Profy, A.T., and Wilson, I.A. (1994). Crystal structure of the principal neutralization site of HIV-1. Science *264*, 82–85.
10. Rini, J.M., Stanfield, R.L., Stura, E.A., Salinas, P.A., Profy, A.T., and Wilson, I.A. (1993). Crystal structure of a human immunodeficiency virus type 1 neutralizing antibody, 50.1, in complex with its V3 loop peptide antigen. Proc. Natl. Acad. Sci. USA *90*, 6325–6329.
11. Stanfield, R., Cabezas, E., Satterthwait, A., Stura, E., Profy, A., and Wilson, I. (1999). Dual conformations for the HIV-1 gp120 V3 loop in complexes with different neutralizing Fabs. Structure *7*, 131–142.

12. Tugarinov, V., Zvi, A., Levy, R., and Anglister, J. (1999). A cis proline turn linking two beta-hairpin strands in the solution structure of an antibody-bound HIV-1IIIB V3 peptide. Nat. Struct. Biol. *6*, 331–335.
13. Myers, G., Foley, B., Mellows, J., Korber, B., Jeang, K., and Wain-Hobson, S. (1996). Human Retroviruses and AIDS: A Compilation and Analysis of Nucleic Acid and Amino Sequences. (Los Alamos, NM: Los Alamos National Laboratory).
14. Nyambi, P.N., Gorny, M.K., Bastiani, L., van der Groen, G., Williams, C., and Zolla-Pazner, S. (1998). Mapping of epitopes exposed on intact human immunodeficiency virus type 1 (HIV-1) virions: a new strategy for studying the immunologic relatedness of HIV-1. J. Virol. *72*, 9384–9391.
15. Cecilia, D., KewalRamani, V.N., O'Leary, J., Volsky, B., Nyambi, P., Burda, S., Xu, S., Littman, D.R., and Zolla-Pazner, S. (1998). Neutralization profiles of primary human immunodeficiency virus type 1 isolates in the context of coreceptor usage. J. Virol. *72*, 6988–6996.
16. Conley, A.J., Gorny, M.K., Kessler, J.A., Boots, L.J., Ossorio-Castro, M., Koenig, S., Lineberger, D.W., Emini, E.A., Williams, C., and Zolla-Pazner, S. (1994). Neutralization of primary human immunodeficiency virus type 1 isolates by the broadly reactive anti-V3 monoclonal antibody, 447–52D. J. Virol. *68*, 6994–7000.
17. Fouts, T.R., Binley, J.M., Trkola, A., Robinson, J.E., and Moore, J.P. (1997). Neutralization of the human immunodeficiency virus type 1 primary isolate JR-FL by human monoclonal antibodies correlates with antibody binding to the oligomeric form of the envelope glycoprotein complex. J. Virol. *71*, 2779–2785.
18. Gorny, M.K., Williams, C., Volsky, B., Revesz, K., Cohen, S., Polonis, V.R., Honnen, W.J., Kayman, S.C., Krachmarov, C., Pinter, A., et al. (2002). Human monoclonal antibodies specific for conformation-sensitive epitopes of V3 neutralize human immunodeficiency virus type 1 primary isolates from various clades. J. Virol. *76*, 9035–9045.
19. Hioe, C.E., Xu, S., Chigurupati, P., Burda, S., Williams, C., Gorny, M.K., and Zolla-Pazner, S. (1997). Neutralization of HIV-1 primary isolates by polyclonal and monoclonal human antibodies. Int. Immunol. *9*, 1281–1290.
20. Verrier, F., Nadas, A., Gorny, M.K., and Zolla-Pazner, S. (2001). Additive effects characterize the interaction of antibodies involved in neutralization of the primary dualtropic human immunodeficiency virus type 1 isolate 89.6. J. Virol. *75*, 9177–9186.
21. VanCott, T.C., Bethke, F.R., Polonis, V.R., Gorny, M.K., Zolla-Pazner, S., Redfield, R.R., and Birx, D.L. (1994). Dissociation rate of antibody-gp120 binding interactions is predictive of V3-mediated neutralization of HIV-1. J. Immunol. *153*, 449–459.
22. Creighton, T.E. (1995). Proteins, Structures and Molecular Properties (New York: W.H. Freeman).
23. Thompson, J., Pope, T., Tung, J.S., Chan, C., Hollis, G., Mark, G., and Johnson, K.S. (1996). Affinity maturation of a high-affinity human monoclonal antibody against the third hypervariable loop of human immunodeficiency virus: use of phage display to improve affinity and broaden strain reactivity. J. Mol. Biol. *256*, 77–88.
24. Wuthrich, K. (1986). NMR of Proteins and Nucleic Acids (New York: John Wiley).
25. Kleywegt, G.J. (1999). Recognition of spatial motifs in protein structures. J. Mol. Biol. *285*, 1887–1897.
26. LaRosa, G.J., Davide, J.P., Weinhold, K., Waterbury, J.A., Profy, A.T., Lewis, J.A., Langlois, A.J., Dreesman, G.R., Boswell, R.N., Shadduck, P., et al. (1990). Conserved sequence and structural elements in the HIV-1 principal neutralizing determinant. Science *249*, 932–935.
27. Gao, G.F., Tormo, J., Gerth, U.C., Wyer, J.R., McMichael, A.J., Stuart, D.I., Bell, J.I., Jones, E.Y., and Jakobsen, B.K. (1997). Crystal structure of the complex between human CD8alpha(alpha) and HLA-A2. Nature *387*, 630–634.
28. Leahy, D.J., Axel, R., and Hendrickson, W.A. (1992). Crystal structure of a soluble form of the human T cell coreceptor CD8 at 2.6 Å resolution. Cell *68*, 1145–1162.
29. Zhang, Z., Lee, C.H., Mandiyan, V., Borg, J.P., Margolis, B., Schlessinger, J., and Kuriyan, J. (1997). Sequence-specific recognition of the internalization motif of the Alzheimer's amyloid precursor protein by the X11 PTB domain. EMBO J. *16*, 6141–6150.
30. Czaplewski, L.G., McKeating, J., Craven, C.J., Higgins, L.D., Appay, V., Brown, A., Dudgeon, T., Howard, L.A., Meyers, T., Owen, J., et al. (1999). Identification of amino acid residues critical for aggregation of human CC chemokines macrophage inflammatory protein MIP-1alpha, MIP-1beta, and RANTES. Characterization of active disaggregated chemokine variants. J. Biol. Chem. *274*, 16077–16084.
31. Chung, C.W., Cooke, R.M., Proudfoot, A.E., and Wells, T.N. (1995). The three-dimensional solution structure of RANTES. Biochemistry *34*, 9307–9314.
32. Wells, T.N., Power, C.A., Lusti-Narasimhan, M., Hoogewerf, A.J., Cooke, R.M., Chung, C.W., Peitsch, M.C., and Proudfoot, A.E. (1996). Selectivity and antagonism of chemokine receptors. J. Leukoc. Biol. *59*, 53–60.
33. Hoh, F., Yang, Y.S., Guignard, L., Padilla, A., Stern, M.H., Lhoste, J.M., and van Tilbeurgh, H. (1998). Crystal structure of p14TCL1, an oncogene product involved in T-cell prolymphocytic leukemia, reveals a novel beta-barrel topology. Structure *6*, 147–155.
34. Wilken, J., Hoover, D., Thompson, D.A., Barlow, P.N., McSparron, H., Picard, L., Wlodawer, A., Lubkowski, J., and Kent, S.B. (1999). Total chemical synthesis and high-resolution crystal structure of the potent anti-HIV protein AOP-RANTES. Chem. Biol. *6*, 43–51.
35. Fernandez, E.J., Wilken, J., Thompson, D.A., Peiper, S.C., and Lolis, E. (2000). Comparison of the structure of vMIP-II with eotaxin-1, RANTES, and MCP-3 suggests a unique mechanism for CCR3 activation. Biochemistry *39*, 12837–12844.
36. Dealwis, C., Fernandez, E.J., Thompson, D.A., Simon, R.J., Siani, M.A., and Lolis, E. (1998). Crystal structure of chemically synthesized [N33A] stromal cell-derived factor 1alpha, a potent ligand for the HIV-1 "fusin" coreceptor. Proc. Natl. Acad. Sci. USA *95*, 6941–6946.
37. Ohnishi, Y., Senda, T., Nandhagopal, N., Sugimoto, K., Shioda, T., Nagal, Y., and Mitsui, Y. (2000). Crystal structure of recombinant native SDF-1alpha with additional mutagenesis studies: an attempt at a more comprehensive interpretation of accumulated structure-activity relationship data. J. Interferon Cytokine Res. *20*, 691–700.
38. Wang, W.K., Dudek, T., Essex, M., and Lee, T.H. (1999). Hypervariable region 3 residues of HIV type 1 gp120 involved in CCR5 coreceptor utilization: therapeutic and prophylactic implications. Proc. Natl. Acad. Sci. USA *96*, 4558–4562.
39. Tugarinov, V., Zvi, A., Levy, R., Hayek, Y., Matsushita, S., and Anglister, J. (2000). NMR structure of an anti-gp120 antibody complex with a V3 peptide reveals a surface important for coreceptor binding. Structure *8*, 385–395.
40. Chandrasekhar, K., Profy, A.T., and Dyson, H.J. (1991). Solution conformational preferences of immunogenic peptides derived from the principal neutralizing determinant of the HIV-1 envelope glycoprotein gp120. Biochemistry *30*, 9187–9194.
41. Hansen, J.E., Lund, O., Nielsen, J.O., Brunak, S., and Hansen, J.E. (1996). Prediction of the secondary structure of HIV-1 gp120. Proteins *25*, 1–11.
42. Nardese, V., Longhi, R., Polo, S., Sironi, F., Arcelloni, C., Paroni, R., DeSantis, C., Sarmientos, P., Rizzi, M., Bolognesi, M., et al. (2001). Structural determinants of CCR5 recognition and HIV-1 blockade in RANTES. Nat. Struct. Biol. *8*, 611–615.
43. Kissler, S., Susal, C., and Opelz, G. (1997). Anti-MIP-1alpha and anti-RANTES antibodies: new allies of HIV-1? Clin. Immunol. Immunopathol. *84*, 338–341.
44. Basmaciogullari, S., Babcock, G.J., Van Ryk, D., Wojtowicz, W., and Sodroski, J. (2002). Identification of conserved and variable structures in the human immunodeficiency virus gp120 glycoprotein of importance for CXCR4 binding. J. Virol. *76*, 10791–10800.
45. Sakaida, H., Hori, T., Yonezawa, A., Sato, A., Isaka, Y., Yoshie, O., Hattori, T., and Uchiyama, T. (1998). T-tropic human immunodeficiency virus type 1 (HIV-1)-derived V3 loop peptides directly bind to CXCR-4 and inhibit T-tropic HIV-1 infection. J. Virol. *72*, 9763–9770.
46. Verrier, F., Borman, A.M., Brand, D., and Girard, M. (1999). Role

of the HIV type 1 glycoprotein 120 V3 loop in determining coreceptor usage. AIDS Res. Hum. Retroviruses *15*, 731–743.

47. Gorny, M.K., Xu, J.Y., Karwowska, S., Buchbinder, A., and Zolla-Pazner, S. (1993). Repertoire of neutralizing human monoclonal antibodies specific for the V3 domain of HIV-1 gp120. J. Immunol. *150*, 635–643.
48. Kuloglu, E.S., McCaslin, D.R., Markley, J.L., and Volkman, B.F. (2002). Structural rearrangement of human lymphotactin, a C chemokine, under physiological solution conditions. J. Biol. Chem. *277*, 17863–17870.
49. Sharon, M., Gorlach, M., Levy, R., Hayek, Y., and Anglister, J. (2002). Expression, purification, and isotope labeling of a gp120 V3 peptide and production of a Fab from a HIV-1 neutralizing antibody for NMR studies. Protein Expr. Purif. *24*, 374–383.
50. Kessler, N., Zvi, A., Ji, M., Sharon, M., Rosen, O., Levy, R., Gorny, M., Zolla-Pazner, S., and Anglister, J. Expression purification and isotope labeling of the Fv fragmnet of the human HIV-1 neutralizing antibody 447-52D for NMR studies. Protein Expr. Purif., in press.
51. Kay, L.E., Nicholson, L.K., Delaglio, F., Bax, A., and Torchia, D.A. (1992). Pulse sequences for removal of the effects of cross-correlation between dipolar and chemical-shift anisotropy relaxation mechanism on the measurement of heteronuclear T1 and T2 values in proteins. J. Magn. Reson. *97*, 359–375.
52. Sattler, M., Schleucher, J., and Griesinger, C. (1999). Heteronuclear multidimensional NMR experiments for the structure determination of proteins in solution employing pulsed field gradients. Prog. Nucl. Magn. Res. Spectrosc. *34*, 93–158.
53. Pervushin, K. (2000). Impact of transverse relaxation optimized spectroscopy (TROSY) on NMR as a technique in structural biology. Q. Rev. Biophys. *33*, 161–197.
54. Vuister, G.W., and Bax, A. (1993). Quantitative J correlation—a new approach for measuring homonuclear 3-bond J(H(N)H (Alpha)) coupling-constants in N-15-enriched proteins. J. Am. Chem. Soc. *115*, 7772–7777.
55. Roberts, G.C.K. (1993). NMR of Macromolecules (New York: Oxford University Press).
56. Cornilescu, G., Delaglio, F., and Bax, A. (1999). Protein backbone angle restraints from searching a database for chemical shift and sequence homology. J. Biomol. NMR *13*, 289–302.
57. Delaglio, F., Grzesiek, S., Vuister, G.W., Zhu, G., Pfeifer, J., and Bax, A. (1995). NMRPipe: a multidimensional spectral processing system based on UNIX pipes. J. Biomol. NMR *6*, 277–293.
58. Neidig, K.-P., Geyer, M., Gorler, A., Antz, C., Saffrich, R., Beneicke, W., and Kalbitzer, H. (1995). AURELIA, a program for computer-aided analysis of multidimensional NMR spectra. J. Biomol. NMR *6*, 255–270.
59. Brunger, A.T., Adams, P.D., Clore, G.M., DeLano, W.L., Gros, P., Grosse-Kunstleve, R.W., Jiang, J.S., Kuszewski, J., Nilges, M., Pannu, N.S., et al. (1998). Crystallography and NMR system: a new software suite for macromolecular structure determination. Acta Crystallogr. D Biol. Crystallogr. *54*, 905–921.
60. Koradi, R., Billeter, M., and Wuthrich, K. (1996). MOLMOL: a program for display and analysis of macromolecular structures. J. Mol. Graph. *14*, 51–55, 29–32.
61. Laskowski, R.A., Rullmannn, J.A., MacArthur, M.W., Kaptein, R., and Thornton, J.M. (1996). AQUA and PROCHECK-NMR: programs for checking the quality of protein structures solved by NMR. J. Biomol. NMR *8*, 477–486.